

Preparation, characterization and photo-inactivation of cellulose nanocrystals impregnated with meso-tetrakis(4-nitrophenyl)porphyrin

Fatemeh Fayyaz^{a,*}, Mahboubeh Rabbani^b, Rahmatollah Rahimi^b, Mehdi Rassa^c

^aDepartment of Science, Payame Noor University (PNU), P.O. BOX 19395-3697 Tehran, Iran

^bBioinorganic chemistry laboratory, Department of Chemistry, Iran University of Science and Technology, Narmak, Tehran, 16846-13114, Iran.

^cDepartment of Biology, Faculty of Science, Guilan University, Rasht, Iran

Received: 30 January 2017, Accepted: 18 November 2017, Published: 18 November 2017

Abstract

In this study, cellulose nanocrystals (CNC) was prepared and meso-tetrakis(4-nitrophenyl)porphyrin (TNPP) was immobilized on it. The product was identified by techniques of UV-Vis, fourier transform infrared (FT-IR), diffuse reflectance UV-Vis spectroscopy (DRS), energy-dispersive X-ray spectroscopy (EDX) and scanning electron microscopy (SEM). The effect of an amount of a loaded porphyrin compound containing the nitro group on CNC was investigated against a typical Gram negative bacterium, *Pseudomonas aeruginosa*, and a typical Gram positive bacterium, *Bacillus subtilis*, under visible light irradiation. The results indicated that CNC incorporated with 14.9% TNPP has a good effect on the photo-inactivation of *P. aeruginosa* and can be used in the textile, biomedicine, biomaterials engineering, membranes and polymer nanocomposites.

Keywords: *Bacillus subtilis*; binding test; cellulose nanocrystals; photodynamic antimicrobial chemotherapy; *Pseudomonas aeruginosa*; TNPP.

Introduction

Cellulose is the main component of natural fibers such as cotton, flax, hemp, jute and sisal [1]. Cellulose microfibrils can be found as intertwined microfibrils in the cell wall depending on its source containing 500–15000 glucose. As well as these microfibrils, there exist cellulose nanocrystals (CNC) which are elongated, flat and few hundreds of nanometers long, 10–20 nm wide and a few nm thick [2].

Cellulose can be used as a polymer for incorporating different materials

used in a variety of applications such as antibacterial surfaces. These surfaces can be developed by grafting quaternary ammonium salts, molecularly engineered peptides, N-halamines or compounds releasing bactericidal moieties such as metal ions or can be consisted of designing photoactive surfaces by incorporating photo-sensitizer materials into coating polymers. It has been shown that porphyrins and related compounds can be used in photodynamic antimicrobial chemotherapy (PACT) and retain their

*Corresponding author: Fatemeh Fayyaz

Tel: +98 (28) 33336366, Fax: +98 (28) 333440481

E-mail: f.fayyaz@yahoo.com

photo-antimicrobial properties when grafted on films or membranes, nanoparticles or polymers [3-6].

Porphyrin compounds are important instances of macrocyclic complexes and have attracted much interest in the study of various processes. These compounds have low toxicity, as they are easily cleared from blood fluids and tissues. Also, they are efficient generators of reactive oxygen species due to absorption of photons in the visible region. Hence, one of the applications of porphyrins, is photodynamic therapy (PDT). In this method, the porphyrins concentrated in tumor cells for destroying of malignant cells, upon illumination in the presence of oxygen [7].

Also, photodynamic antimicrobial chemotherapy (PACT) is a developmental therapeutic option that applies visible light to photosensitive molecules to induce oxidative damage to microbial pathogens *via* the production of reactive oxygen species [8-10].

Some nitro-containing compounds such as nitrofurans and nitroimidazoles are operative antibacterial agents and are used extensively to battle anaerobic and protozoal infections [11]. Nitro-substituted aromatic compounds have been found to be effective electron-affinity radio-sensitizers. Nitro and amino groups can be easily functionalized and conjugated with bioactive molecules, such as monoclonal antibodies, oligomeric carboranyl phosphate diesters, polymer backbones, and cyclodextrins [12,13]. Porphyrins substituted with electron-withdrawing groups, such as nitro group(s), have been studied for tuning redox and photo-physical properties and for further functionalization of the macrocycle [14]. Various approaches

were used for photo-inactivation of porphyrin compounds in many articles [15-19]. At previous work [20], cellulosic fabrics have impregnated with tetracationic porphyrins and the products have effective photo-inactivation effect against common bacteria. In this research, we prepared porphyrin with substituent nitro groups (with-drawing group) and incorporated to CNC. For this purpose, tetrakis(4-nitrophenyl)porphyrin (TNPP) compound and cellulose nanocrystals (CNC) have been synthesized and various proportions of TNPP/CNC were prepared and the photo-inactivation properties of the prepared TNPP and TNPP/CNC were considered.

Experimental

General

All chemicals were purchased from Merck Company and used without further purification. Pyrrole was distilled under vacuum.

UV-Vis absorption spectra were recorded on a UV-1700 pharma spectrometer Shimadzu. The FT-IR measurements were carried out with the help of Shimadzu FT-IR spectrometer in the form of KBr pellets. ¹H NMR spectra were obtained at 300 MHz (Bruker) instrument. DRS spectra were obtained using a Shimadzu (MPC-2200) spectrophotometer. The surface morphology of CNC was observed by SEM using a VEGA\\TESCAN scanning microscope. Electron micrographs of the sample were recorded at 600× magnification. The energy dispersive X-ray spectroscopy (EDX) is taken with a Philips (XL-30) to prove the elemental presence. Ultrasonication was done with Elma 500 W ultrasonic homogenizer. A Samsung domestic microwave was used for microwave irradiation. A 100

Watt tungsten lamp was used as light source, placed at a distance of 20 cm from the sample. To absorb heat, a plate filled with water was used. This system was setup in a shaker incubator at a rate of 80 rpm. All the experiments were carried out in a dark room to avoid light reflection.

Synthesis meso-tetrakis(4-nitrophenyl)porphyrin

TNPP was synthesized by microwave irradiation similar to the article [21]. Briefly, (0.01mol) 4-nitrobenzaldehyde, (0.01mol) pyrrole, Lactic acid (2 mL) and nitrobenzene (30 mL) were mixed in a 100 mL Erlenmeyer flask. The flask was then transferred to a microwave and cooked for 15 minutes at 280 watts. Every 2 minutes, the flask was taken out and shaken. After completion, the reactants were cooled to room temperature. Purple crystals were separated by suction filtration and small amount of CH₃OH (about 20 mL) was added to the mixture and shaken vigorously. This mixture was allowed to stand overnight, then washed using a mixture of CH₂Cl₂ and C₂H₅OH (1:1). The purity of the product was confirmed by TLC. The crystals were vacuum dried (product yield was 30 %).¹HNMR (CDCl₃) δ: -2.73 (s, 2NH); 7.76, 8.24 (d, J = 5.5 Hz, 16H, C₆H₄); 8.87 (S, 8H, β-Pyrrole).UV-Vis in DMF (λ_{max}, nm): 423, 516, 551, 591, 646 nm.

Synthesis of cellulose nanocrystals (CNC)

The cellulose nanocrystals were formed by acidic hydrolysis as reported in the article with little changes [22]. Briefly, 2.0 g of cellulose pulp were obtained from Whatman #1 filter paper (98% α-cellulose, 80% crystalline) and blended in a Blender. Hydrolysis of the resulting pulp were achieved after 3 h at

100 °C using 100 mL of 2.5 M HBr and intermittent ultrasonication (5 min per hour). After dilution with de-ionized water, the mixture was subjected to five washing/centrifugation cycles (5000g, 10 min) to remove excess acid and water-soluble fragments. Once pH reached 4-5, the fine cellulose particles started to disperse into the aqueous supernatant. The polydisperse cellulose contained in the turbid supernatant was collected and subjected to centrifugation at 15,000g for 60 min in a superspeed centrifuge to remove ultrafine particles. The sediment contained the cellulose nanocrystals and was dried at lab temperature.

Incorporation of TNPP on CNC

The porphyrin solutions were prepared in DMF at concentrations of 2.5×10⁻⁴(product 1), 5×10⁻⁴(product 2) and 7.5×10⁻⁴ M (product 3), and 0.005g CNC were impregnated with these solutions at 60 °C for 24 h. After that, the products were washed with DMF. Washing cycles were done to remove unbound photo-sensitizers. These cycles were repeated until washing solutions did not show any trace of porphyrins using UV-Vis spectrophotometer. The amount of porphyrin grafted to CNC was calculated by spectrophotometer. The absorbance of porphyrin was recorded at the beginning and the end of the reaction. Also, according to the following equation, the percent of porphyrin on CNC was calculated:

$$\frac{\text{The amount of porphyrin grafted}}{\text{The amount of CNC}} \quad \text{The percent of porphyrin on CNC =} \quad \text{(Equation 1)}$$

Photo-inactivation of bacteria on agar surface

Bacillus subtilis and *Pseudomonas aeruginosa* were obtained from the microbiology laboratory of Guilan University. The strains were grown in

nutrient broth or nutrient agar overnight at 37 °C. 30 µL of these broths were aseptically transferred onto nutrient agar plates and spread on the surface with a sterile spreader. Wells (diameter 0.5 cm) were made in nutrient agar seeded with the target strain, using sterile Pasteur pipette ends. A stock solution of TNPP was prepared in pure DMF at various concentrations. Aliquots of 30 µL of different concentrations of porphyrin were added to these wells. The plates were incubated at 37 °C for 20 minutes in the dark and illuminated for 30 minutes. They were then incubated at 37 °C overnight in the dark. One well was filled with DMF in the same conditions, as negative control. Another test was also employed using porphyrins not photo-activated with light source. The experiments were carried out in triplicate. Bacterial growth was examined visually by measuring inhibition zones around the wells. A diameter larger than 10 mm was considered as a positive response formally. A negative control test was done with TNPP on the CNC against the bacteria at the dark condition. For this aim, a little amount of them (0.005 g) weight and added into plates and one well was placed CNC in the same conditions.

Photo-inactivation of bacteria in broth

30 µL of bacterial suspension (~10⁹ cfu/mL) and various concentrations of porphyrin were added to nutrient broth and incubated for 20 min under dark conditions at 37 °C in order for the porphyrins to bind to the bacteria. The cultures were then illuminated for 30 minutes with the light source and incubated overnight. Then, 100 µL of culture was spread onto the surface of a nutrient agar plate and incubated at 37

°C overnight. This experiment was repeated three times.

Binding test of porphyrins to bacteria

This procedure was done according to our previous article [23]. Briefly, thirty milliliters of bacterial suspension (~3×10⁷ cfu/mL) was supplemented with TNPP at a concentration of 1.2 µM (with DMF) in nutrient broth and the sample were centrifuged (10,000 rpm for 1 minute). The visible spectra of the supernatants were recorded at time zero and after 20 minutes incubation at 37 °C under dark conditions. The percent binding of porphyrin to the bacterial cells was obtained by using a UV-Vis spectrophotometer and decreasing absorption of porphyrins at the Soret band. This experiment was repeated three times and the binding of TNPP of the bacteria was expressed as a percentage.

Results and discussion

The preparation of nanocellulose was done at acidic hydrolysis. Figure 1a shows polydisperse of nanocellulose in the middle part of media at pH=4-5 at the right of the graph. The middle phase was collected and subjected by centrifugation at 14000 RPM for 60 min in a high speed centrifuge to remove very fine particles. Cellulose nanocrystals was collected and dried at lab temperature.

DRS analysis led to approximately similar spectra to UV-Vis porphyrin in solution: Soret band at 423 nm and Q bands between 500-700 nm clearly were shown up. According to Figure 1a, the appearance of Q bands implies that the surface of the conjugated CNC did not contain any distortions. Upon grafting the TNPP onto CNC, Soret bands broadened. This can be attributed

to π -electron interaction with hydroxyl groups of CNC. DRS analyses confirm that TNPP is attached onto the CNC surface and show interaction between them.

The FT-IR spectra of TNPP, CNC and TNPP/CNC were recorded and shown in (Figure1b). For FT-IR spectrum of TNPP, the peaks present at 699.94 cm^{-1} shows the presence of γ CH meso phenyl; the short peak at 1518 cm^{-1} is probably due to the presence of NH groups in the porphyrin structure; the peak at 1474 cm^{-1} is due to the presence of the aromatic skeleton; the peak at 1695 cm^{-1} is due

to the presence of ring C=N; the peaks around 1520 cm^{-1} and 1340 cm^{-1} indicates the presence of nitro groups. Short peaks around 1515 cm^{-1} may be due to NH groups and peak at 1473 cm^{-1} is due to the presence of aromatic rings [24]. For CNC and CNC/TNPP, spectral data have been found: 3340 cm^{-1} (OH is stretching), 2850 and 2900 cm^{-1} (symmetric and asymmetric C-H is stretching), 1325 , and 1045 cm^{-1} (C-O stretching) [25-28]. The change frequency at range $1000\text{-}2000\text{ cm}^{-1}$ for CNC/TNPP shows that TNPP has interaction with hydroxyl groups in CNC.

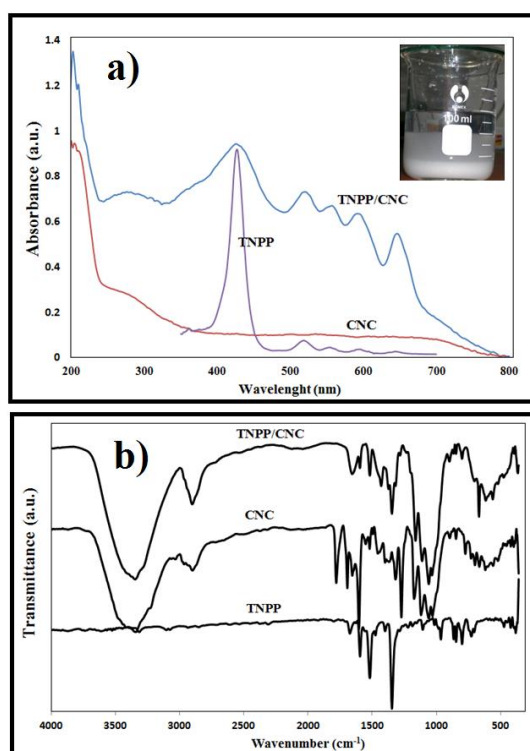


Figure 1. The polydisperse of nanocellulose at middle part of media. a) The DRS of CNC and CNC/TNPP and UV-Vis spectra of pure TNPP in DMF. b) The FT-IR spectra of pure TNPP, CNC and TNPP/CNC

The surface of untreated CNC and CNC/TNPP was examined by scanning electron microscopy (SEM). Typical scanning electron photomicrographs are presented in Figure 2. The nanocrystal of cellulose is recognized in this figure.

Also, the EDX analysis was used for determination of elementals of CNC qualitatively. A correct elemental analysis of CNC with EDX is not possible. According to this analysis, the maximum weight percent of CNC was

carbon and oxygen. Also, there is a little sulfur in this compound that can

be attributed to filter paper.

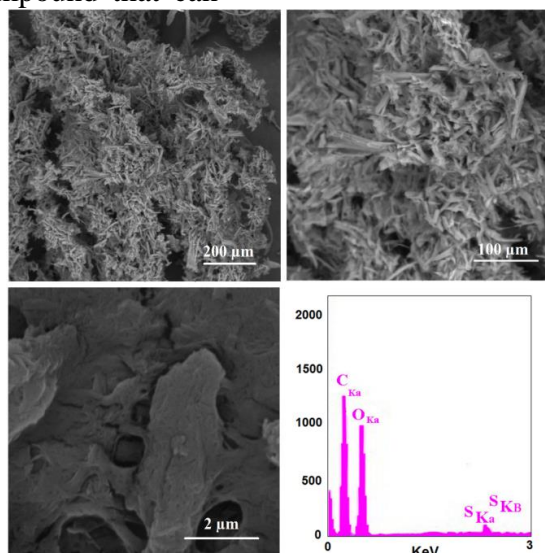


Figure 2. The SEM images and the EDX of CNC

According to the results of the techniques FT-IR, SEM and DRS, it is clear that TNPP was attached to CNC with electrostatic interactions between nitro groups in TNPP and hydroxyl groups of CNC. This interaction caused changing in frequency at the range of $1000\text{-}2000\text{ cm}^{-1}$ for CNC/TNPP and CNC.

The effect of various concentrations of TNPP against two strains of bacteria on agar surface are shown in Table 1. The plates containing inactivated porphyrins did not show any photo-inactivation of the bacteria, with complete growth over the agar surface. Also, the effect of various concentrations of TNPP on $\log(\text{cfu/mL})$ of two strains of bacteria after overnight incubation was shown in Table 2.

The effect of various proportions of TNPP/CNC against *B. subtilis* and *P. aeruginosa* were done and shown in Table 3. This table showed that product 2 can be affected against *P. aeruginosa*

with percent of 14.9% of porphyrin. To consider the photo-inactivation property of TNPP/CNC, 0.005 g of this product was weighed and placed on the agar surface. Pure CNC was put on one well for negative control. Inhibition zones, shown in Figure 3, larger than 10 mm, were considered as a positive response formally. As shown in Table 1, TNPP was more effective against *P. aeruginosa* than *B. subtilis*. Also, the percent of photo-inactivation of bacteria by this compound was shown in this table. As shown in Figure 3, the inhibition was completely inside the zone for *P. aeruginosa*, sporadic colonies of *B. subtilis* started growing inside the inhibition zones, which clearly indicated the rapid emergence of resistant *B. subtilis* strain. The results of Table 3 showed that incorporation of TNPP to CNC is more effective against *P. aeruginosa* than *B. subtilis* for products 2 and 3. Also, the inhibition zone of TNPP/CNC was shown in Figure 3.

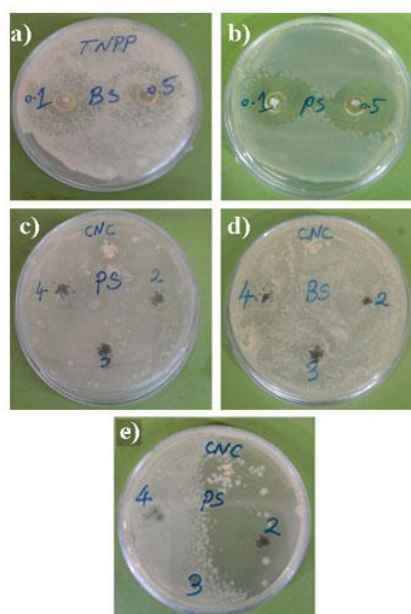


Figure 3. The effect of TNPP and TNPP/CNC against *B. subtilis* and *P. aeruginosa*. (a) TNPP with *B. subtilis*; (b) TNPP with *P. aeruginosa*; (c) negative control of the samples in dark condition against *P. aeruginosa*; (d) TNPP / CNC against *B. subtilis* and (e) TNPP/CNC against *P. aeruginosa*

Table 1. The effect of TNPP against two strains of bacteria on agar surface

Porphyrin concentration (µg/well)	size of hole(mm)	size of hole(mm)	% Photo-inactivation	% Photo-inactivation
	<i>P. aeruginosa</i>	<i>B. subtilis</i>	of <i>P. aeruginosa</i>	of <i>B. subtilis</i>
60	19(±1) ‡	20*(±1) ‡	22.6(±2) ‡	8.24(±1.5) ‡
45	18(±1) ‡	20*(±1) ‡	21.9(±1.9) ‡	7.8(±1.6) ‡
30	15(±1) ‡	19*(±1) ‡	21.3(±1.6) ‡	7.5(±1.6) ‡
10	11(±1) ‡	19*(±1) ‡	10.6(±1.3) ‡	6(±1.8) ‡

*A number of colonies started growing around the wells.

‡Standard deviation measured for 3 experimental

Table 2. The effect of various concentrations of TNPP on log (cfu/mL) of two strains of bacteria after overnightincubation

Concentration (µg/mL)	<i>P. aeruginosa</i>	<i>B. subtilis</i>
	TNPP log(cf/mL)	TNPP log(cf/mL)
10 µg/mL	8.25(±0.237) ‡	7.75(±0.075) ‡
30 µg/mL	7.26(±0.370) ‡	7.67(±0.085) ‡
60µg/mL	7.14(±0.150) ‡	7.57(±0.110) ‡
Untreated	9.23(±0.204) ‡	8.25(±0.237) ‡

‡Standard deviation measured for 3 experimental

Table 3. The effect of TNPP on CNC against bacteria cells immobilized on agar surface

Products	The percent of grafted porphyrin	size of hole(mm)	size of hole(mm)
		<i>P. aeruginosa</i>	<i>B. subtilis</i>
product 3	27.6	12(±1) ‡	5(±1) ‡
product 2	14.9	11(±1) ‡	5(±1) ‡
product 1	8.7	5(±1) ‡	5(±1) ‡
CNC	-	-	-

‡Standard deviation measured for 3 experimental

According to our experiments, TNPP was more effective in photo-inactivation of *P. aeruginosa* than *B. subtilis*. Binding tests can be used to confirm this point, as described above. According to this experimental results, the percentage binding of TNPP to *B. subtilis* and *P. aeruginosa* was 1.89%, 16.78% respectively. It can be argued that the percentage binding of *P. aeruginosa* to TNPP is more than other strains.

At the end of this sequence, the porphyrin molecule returns to the ground state and $^1\text{O}_2$ is formed [4, 28-30]. The production of $^1\text{O}_2$ plays an important role in the mechanism of the action of porphyrins under light conditions. This molecule is able to react with almost every cellular ingredient, bringing about the irreversible damage that ultimately leads to cell death [31].

According to the results of antibacterial tests of treated cellulose, the production of $^1\text{O}_2$ plays an important role in the mechanism of action of porphyrins under light conditions. Clearly, the exact mechanism of action of porphyrin compounds needs further investigation. It seems that various factors could affect this mechanism, such as binding and the concentration of the photosensitizer, morphology of bacteria, and illumination time.

In this work, TNPP/CNC was an effective product in photo-inactivation of *P. aeruginosa*, but in comparison with the previous work [20], it showed less effective photo-inactivation. This can be attributed to the low solubility of TNPP and its less linkage to bacteria.

Conclusion

In this study, TNPP, CNC and TNPP/CNC were prepared and identified by techniques of UV-Vis, FT-IR, DRS, EDX and SEM. The application of these products was done in microbiology area and against *B. subtilis* and *P. aeruginosa* with a tungsten lamp (100W) and illumination time was 30 min. The results indicate that TNPP and TNPP/CNC have efficiency for photo-inactivation of Gram negative bacterium *P. aeruginosa* rather than *B. subtilis*. On the other hands, CNC has unique properties such as mechanical, optical and surface area and it's utilized in textile, biomedicine, biomaterials engineering, membranes and polymer nanocomposites. So, incorporation of TNPP to CNC with a ratio of 5:2 can be prepared to use as coverage with property photo-inactivation minimal against *P. aeruginosa*.

Acknowledgments

The authors are grateful to Iran University of Science and Technology

for partial assistance of this research project.

References

- [1] J.I. Moran, V.A. Alvarez, V.P. Cyras, A. Vazquez, *Cellulose*, **2008**, *15*, 149–159.
- [2] Y. Zhang Xiao-Bin Lu, C. Gao, Wei-Jun Lv, Ju-Ming Yao, *Journal of Fiber Bioengineering & Informatics*, **2012**, *5*, 263–271.
- [3] C. Ringot, V. Sol, R. Granet, P. Krausz, *Materials Letters*, **2009**, *63*, 1889–1891.
- [4] N. Drogat, R. Granet, C. Le Morvan, G. Bégaud-Grimaud, P. Krausz, V. Sol, *Bioorganic & Medicinal Chemistry Letters*, **2012**, *22*, 3648–3652.
- [5] J.P. Mbakidi, K. Herke, S. Alves, V. Chaleix, R. Granet, P. Krausz, S. Leroy-Lhez, T.S. Ouk, V. Sol, *Carbohydrate Polymers*, **2013**, *91*, 333–338.
- [6] C. Ringot, V. Sol, M. Barrière, N. Saad, P. Bressollier, R. Granet, P. Couleaud, C. Frochot, P. Krausz, *Biomacromolecules*, **2011**, *12*, 1716–1723.
- [7] X.Y. Liu, H.M. Wang, J.Q. Jiang, J.H. Xiao, R.L. Gao, F.Y. Lin, *Chemico-Biological Interactions*, **2008**, *172*, 154–158.
- [8] S. Banfi, E. Caruso, L. Buccafurni, V. Battini, S. Zazzaron, P. Barbieri, V. Orlandi, *Journal of photochemistry and photobiology B Biology*, **2006**, *85*, 28–38.
- [9] C.M. Cassidy, R.F. Donnelly, M.M. Tunney, *Journal of Photochemistry & Photobiology, B: Biology*, **2010**, *99*, 62–66.
- [10] A. Peèkaitytė, R. Daugelaviėiusa, A. Sadauskaitė, V. Kirvelienė, R. Bonnett, E. Bakienė, **2005**, No.1, 41–46.
- [11] E.V. Alopina, T.A. Ageeva, A.V. Lyubimtse, O.Yu. Kuznetsov, S.A. Syrbu, Os.I. Koifman, *Macroheterocycles*, **2012**, *5*, 76–80.
- [12] R. Luguya, L. Jaquinod, F.R. Fronczek, M. Graca, H. Vicente, K.M. Smith, *Tetrahedron*, **2004**, *60*, 2757–2763.
- [13] M.A. Schiavon, L.S. Iwamoto, A.G. Ferreira, Y. Iamamoto, M.V. B. Zanoni and M.das D. Assis, *J. Braz. Chem. Soc.*, **2000**, *11*, 458–466.
- [14] K. Rajesh, A. Kalilur Rahiman, K. Shanmuga Bharathi, S. Sreedaran, V. Gangadevi, V. Narayanan, *Bull. Korean Chem. Soc.*, **2010**, *31*, 2656–2664.
- [15] J. Zhang, X. Wu, X. Cao, F. Yang, J. Wang, X. Zhou, X. Lian Zhang, *Bioorganic & Medicinal Chemistry Letters*, **2003**, *13*, 1097–1100.
- [16] H. Ashkenazi, Y. Nitzan, D. Ga, *Photochemistry and Photobiology*, **2003**, *77*, 186–191.
- [17] V. Sol, P. Branland, V. Chaleix, R. Granet, M. Guilloton, F. Lamarche, B. Verneuil, P. Krausz, *Bioorganic & Medicinal Chemistry Letters*, **2004**, *14*, 4207–4211.
- [18] D. Lazzeri, M. Rovera, L. Pascual, E.N. Durantini, *Photochemistry and Photobiology*, **2004**, *80*, 286–293.
- [19] V.T. Orlandi, E. Caruso, S. Banfi, P. Barbieri, *Photochemistry and Photobiology*, **2012**, *88*, 557–564.
- [20] R. Rahimi, F. Fayyaz, M. Rassa, *Materials Science and Engineering C*, **2016**, *59*, 661–668.
- [21] R. Rahimi, F. Fayyaz, M. Rassa, M. Rabbani, *Iranian Chemical Communication*, **2016**, *4*, 175–185.
- [22] E. Feese, H. Sadeghifar, H.S. Gracz, D.S. Argyropoulos, R.A. Ghiladi, *Biomacromolecules*, **2011**, *12*, 3528–3539.
- [23] F. Fayyaz, R. Rahimi, M. Rassa, A. Maleki, *Water Science & Technology: Water Supply*, **2015**, *15*(5), 1099–1105.
- [24] T. Kangwanwong, W. Pluempanupat, W. Parasuk, H.E.

- Keenan, A. Songsasen, *ScienceAsia*, **2012**, *38*, 278–282.
- [25] A. Allen, J. Foulk, G. Gamble, *J. Cotton Sci.*, **2007**, *11*, 68–74.
- [26] J. Alongi, C. Colleoni, G. Rosace, G. Malucell, *J. Therm.Anal.Cal.*, **2012**, *110*, 1207–1216.
- [27] C. Chung, M. Lee, E.K. Choe, *Carbohydrate Polymer.*, **2004**, *58*, 417–420.
- [28] R. Dosselli, C. Tampieri, R. RuizGonzález, S.D. Munari, X. Ragàs, D. Sánchez-García, M. Agut, S. Nonell, E. Reddi, M. Gobbo, *J. Med. Chem.*, **2013**, *56*, 1052–1063.
- [29] S. Mordon, C. Cochrane, J.B. Tylcz, N. Betrouni, L. Mortier, V. Koncar, *Photodiag. Photodyn. Therap.*, **2015**, *12*, 1–8.
- [30] S. Senthilkumar, R. Hariharan, A. Suganthi, M. Ashokkumar, M. Rajarajan, K. Pitchumani, *Powder Technology*, **2013**, *237*, 497–505.
- [31] M. Krouit, R. Granet, P. Krausz, *Eur. Polym. J.*, **2009**, *45*, 1250–1259.